Fluorescence of the DNA Double Helix (dA)20×(dT)20 Studied by Femtosecond Spectroscopy-Effect of the Duplex Size on the Properties of the Excited States

D. Onidas, T. Gustavsson, E. Lazzarotto, D. Markovitsi

Fluorescence of the DNA double helix $(dA)_{20}.(dT)_{20}$ studied by femtosecond spectroscopy – effect of the duplex size on the properties of the excited states

Delphine Onidas, Thomas Gustavsson, Elodie Lazzarotto, Dimitra Markovitsi*

Laboratoire Francis Perrin, CEA/DSM/DRECAM/SPAM - CNRS URA 2453, CEA/Saclay, 91191 Gif-sur-Yvette, France

Abstract

The fluorescence of the DNA double stranded oligomer $(dA)_{20}.(dT)_{20}$ is studied at room temperature by fluorescence upconversion at times shorter than 10 ps. The profile of the upconversion spectra is similar to that of the steady-state fluorescence spectrum, showing that the major part of the photons is emitted within the probed time-scale. At all the probed wavelengths, the fluorescence decays are slower than those of the monomeric chromophores dAMP and TMP. The fluorescence anisotropy decays show strong wavelength dependence. These data allows us to conclude that energy transfer takes place in this double helix and that this process involves exciton states. The spectral and dynamical properties of the oligomer are compared to those of the polymer poly(dA).poly(dT), composed of about 2000 base pairs, reported previously. The oligomer absorption spectrum is characterized by a smaller hypsochromic shift and weaker hypochromism compared to the polymer. Moreover, the fluorescence decays of $(dA)_{20}.(dT)_{20}$ are a twice as fast as those of poly(dA).poly(dT) and its fluorescence anisotropy decays more slowly. These differences are the fingerprints of a larger delocalization of the excited states induced by an increase in the size of the duplex.

Introduction

Characterization of the excited states of DNA double helices is an important step towards the understanding of the UV induced damage of the genetic code which may lead to carcinogenic mutations. This subject, which gave rise to numerous studies since the sixties, is currently undegoing a revival, impelled by femtosecond spectroscopy. However, although many articles describe the ultrafast excited state relaxation of the monomeric chromophores (bases, nucleosides and nucleotides), both in aqueous solutions[1-4] and in various solvents,[5-7] the time-resolved investigations performed for double helices with femtosecond resolution are very scare. This is due to both experimental and conceptual difficulties. On the one hand, the damage induced by intense femtosecond pulses to DNA duplexes, either by direct photon absorption or by electrophilic attack from the generated solvated electrons, imposes the use of specific experimental protocols.[8] In this respect, the much higher cost of DNA duplexes compared to the monomeric chromophores is a serious limiting factor. On the other hand, the complexity of such systems makes the interpretation of the experimental results difficult.[9]

The above mentioned studies dealing with DNA duplexes have been performed for model helices composed exclusively by one type of base-pair, adenine-thymine. In 2003, we reported the fluorescence decay of the oligomer $(dA)_{20}.(dT)_{20}$, recorded by the upconversion technique at the maximum of the emission spectrum.[10] It was found to be slower than those obtained for an equimolar mixture of the corresponding nucleotides (dAMP: 2'-deoxyadenosine monophosphate; TMP: thymidine monophosphate) and for each one of the single strands $(dA)_{20}$ and $(dT)_{20}$. Despite this relative lengthening, the average fluorescence lifetime determined for $(dA)_{20}.(dT)_{20}$ at 330 nm is still very short (1.23 ps).[10]

Next, we focused our efforts on the much longer polymer poly(dA).poly(dT), composed of about 2000 base pairs. After femtosecond excitation at 267 nm, we detected fluorescence at various wavelengths, over a large time-domain by means of two different techniques, fluorescence upconversion and time-correlated single photon counting.[11,12] These time-resolved data, associated with the steady-state absorption and fluorescence spectra, lead to the conclusion that the Franck-Condon excited states are delocalized over several bases, in line with results from circular dichroïsm performed on duplexes containing the same base sequence.[13,14] The initial low value and subsequent decrease of fluorescence anisotropy observed for poly(dA).poly(dT), on the subpicosecond time-scale,[11] when molecular motions

are hindered, proved that energy transfer takes place among the bases in less than 100 fs via intraband scattering.

In 2005, Crespo-Hernández et *al.* studied the oligomers $(dA)_{18}.(dT)_{18}$, and $(dAdT)_9.(dAdT)_9$ by transient absorption with femtosecond resolution.[15] The time constant of 150 ps, corresponding to an important part of the signal determined for $(dA)_{18}.(dT)_{18}$ by transient absorption, is about two orders of magnitude larger than that observed for $(dA)_{20}.(dT)_{20}$ by fluorescence upconversion (1.23 ps).[10] The model proposed by Crespo-Hernández et *al.*, involving population of locally excited states and ultrafast formation of excimers, has been the object of further discussion.[9,16] During this discussion, the necessity of studying the fluorescence decays of oligomeric duplexes at various wavelengths was judged to be important for the understanding of the excited state relaxation.[15] In contrast, a quite recent work by Buchvarov et *al.*,[17] reported transient absorption spectra for similar duplexes and detected the fingerprint of exciton states. They concluded that the degree of delocalization may reach ten base pairs.

One important question is up to which point the size of the duplex affects the properties of the excited states. As a matter of fact, X ray diffraction measurements carried out for $(dA)_n.(dT)_n$ oligomers in solution brought clear evidence that configurational broadening is more important for short duplexes.[18] Such an increased structural disorder may limit the degree of delocalization. Buchvarov et *al.*,[17] found indeed a weak difference between $(dA)_{12}.(dT)_{12}$ and $(dA)_{18}.(dT)_{18}$. In this respect, a comparison between oligomeric duplexes and much longer polymeric structures, closer to natural DNA, may be quite informative.

Within this context, we present here a thorough study of $(dA)_{20}.(dT)_{20}$ using the fluorescence upconversion technique. More precisely, we report fluorescence decays and fluorescence anisotropy decays determined at four emission wavelengths as well as time-resolved fluorescence spectra. Our objective is double. On the one hand, we address the question of energy transfer among bases within this oligomer. On the other, we make a quantitative comparison of the results obtained for $(dA)_{20}.(dT)_{20}$ with those published previously for poly(dA).poly(dT).[11]

Experimental methods

Nucleotides, dAMP and TMP, were obtained from Sigma Aldrich. $(dA)_{20}.(dT)_{20}$ was purchased from Eurogentec; it was purified by polyacrylamide gel electrophoresis (PAGE) and delivered as a duplex in phosphate buffer (pH=6.8; 0.1 M NaH_2PO_4, 0.1 M Na_2HPO_4,

0.25 M NaCl). About twelve different batches were used. Typical melting curves are shown in supporting information. In reference [8] (Figure 4) we reported that the duplex contains a fluorescent impurity peaking at 450 nm, whose concentration varies from one batch to another. Eventually, we managed to obtain batches whose spectra are devoid of this second peak. However, we found that the presence of this impurity did not affect the upconversion decays because it is characterized by a nanosecond lifetime.

Steady-state absorption and fluorescence spectra were recorded with a Perkin-Elmer Lamda 900 and a SPEX Fluorolog-2 spectrofluorometer, respectively, according to the procedure described previously.[4]

The fluorescence upconversion set-up is described in detail elsewhere.[2,4,19] The excitation source was the third harmonic of a mode-locked Ti-sapphire laser (50 mW at 267 nm) operating at a repetition rate of 76 MHz. Temporal scans were made in both parallel (I_{par}) and perpendicular (I_{perp}) modes at 310, 330, 380 and 420 nm, by controlling the polarization of the exciting beam with a half-wave plate. The total fluorescence decays F(t), designated hereafter simply as "fluorescence decays", were calculated according to: $F(t) = I_{par}(t) + 2I_{per}(t)$. The apparatus function was *ca*. 400 fs (fwhm) at 330 nm and it decreased slightly with increasing wavelength. The time-resolution of our set-up is judged to be 100 fs after de-convolution in the sense of a lower limit; in other terms, we cannot determine time constants shorter than 100 fs. Spectra were recorded directly by simultaneously scanning the monochromator wavelengths, rotating the upconversion crystal, and changing the delay line position in order to compensate for the group velocity dispersion.[20] In this way, the band width of the time-resolved spectra is not affected by phase matching problems.

About 20 ml of solution were kept flowing through a 0.4 mm quartz cell (optical densities at 267 nm: 0.15 – 0.25), which was in continuous motion perpendicular to the excitation beam. In the absence of flow-cell, successive fluorescence decays became shorter and shorter.[8] The pulse intensity at the surface of the cell was 200 MW/cm^2.

Both steady-state and time-resolved fluorescence spectra were corrected for the spectral response of the detection systems. All measurements were carried out at 20 ± 1°C.

Results

The steady-state fluorescence spectrum of $(dA)_{20}.(dT)_{20}$ recorded following excitation at 267 nm is shown in Figure 1 together with those of poly(dA).poly(dT) and TMP. The maximum of the $(dA)_{20}.(dT)_{20}$ spectrum is located at the same position as that of TMP (330 ± 1 nm) but at somewhat longer wavelength than that of poly(dA).poly(dT), which peaks at 327

± 1 nm. The similarity between the peak position of the fluorescence spectrum of poly(dA).poly(dT), dissolved in sodium cacodylate, with that of TMP, had lead in past to the conclusion that emission of the polymer originates only from excited states localized on thymines.[21,22] In the buffer and salt conditions used in our experiments, this resemblance is even stronger for the oligomer compared to the polymer. The intensity of the $(dA)_{20}.(dT)_{20}$ and the poly(dA).poly(dT) spectra in Figure 1 is representative of their relative fluorescence quantum yield which is higher by 15 ± 5% for the oligomer than for the polymer ($3x10^{-4}$).[11] This difference arises from the fact that the oligomer spectrum is more intense than that of polymer at its red side.

Figure 1

Figure 2 shows the normalized fluorescence decays of $(dA)_{20}.(dT)_{20}$ determined for various emission wavelengths. For all the probed wavelengths, more than 90% of the signal amplitude has decreased at 7 ps. When going from 310 to 330 nm the decay clearly slows down. Upon further increase in the emission wavelength, the behavior of the signal becomes more complex. Thus, the initial part of the signals obtained at 380 and 420 nm is faster than that of the signal 330 nm but a cross-over takes place around 3-4 ps. The fluorescence decays recorded for each one of the monomeric chromophores (dAMP or TMP) do not exhibit any wavelength dependence between 310 and 420 nm.[4]

Figure 2

In order to describe the decays in a quantitative way and compare them to the decays of poly(dA).poly(dT),[11] we performed for both duplexes a non-linear fitting/deconvolution procedure using bi-exponential functions, $F(t) = \alpha.\exp(-t/\tau_1) + (1-\alpha).\exp(-t/\tau_2)$, convoluted with the Gaussian apparatus function. The fitting parameters as well as the average decay time, defined as $\langle\tau_{1-2}\rangle = \alpha.\tau_1 + (1-\alpha).\tau_2$, are given on Table 1. Fits with tri-exponential functions yielded τ_3 values located in the nanosecond time-domain (see supporting information). This third lifetime could be alternatively replaced by a simple constant, as reported in reference.[10] Nanosecond components of weak amplitude have been detected by time-correlated single photon counting.[9]

Table 1

We observe on Table 1 that at, all wavelengths, the τ_1 values are smaller than 1 ps whereas the τ_2 values amount to a few ps. Both time constants increase with increasing wavelength; however this trend is much clearer for τ_2 which is responsible for the cross-over observed in Figure 2. The pre-exponential factors are all positive. Only positive pre-exponential factors were derived also from fits with tri-exponenial functions (see supporting information). This means that the rise time is faster than the resolution of our setup (100 fs).

Table 2

The average lifetimes $<\tau_{1\text{-}2}>$ determined for $(dA)_{20}.(dT)_{20}$ are compared to those derived from the fits of the poly(dA).poly(dT) decays, on Table 2. The polymer values are twice as large than those found for the oligomer. The effect of the duplex size on the fluorescence decays can be observed in a more clear way on Figure 3, where the bi-exponential functions, resulting from the fitting/deconvolution of the experimental decays obtained for each duplex at 330 nm are represented.

Figure 3

The fluorescence anisotropy r(t) determined at the maximum of the emission spectrum for $(dA)_{20}.(dT)_{20}$ is presented in Figure 4 together with the corresponding fluorescence decay. At zero time, defined as the time needed for the fluorescence signal to reach its half intensity, r(0) is equal to 0.31. Then, the anisotropy decreases slowly and, it reaches a value of *ca.* 0.2 at 6 ps.

Figure 4

The anisotropy decays determined at other wavelengths are noisier than that determined at the fluorescence maximum. Therefore, they are shown only on a 3 ps scale (Figure 5). On the right panel of Figure 5, we have plotted the anisotropies obtained for the monomeric chromophores, dAMP and TMP. These are presented only on 1 ps interval because the fluorescence lifetimes of these two nucleotides is only 0.13 ps and 0.64 ps,

respectively.[10] We observe that both the zero time value and the decay pattern of the $(dA)_{20}.(dT)_{20}$ anisotropy depend on the emission wavelength. However, we stress that the signals are not deconvoluted with respect to the instrumental response function.

Figure 5

In order to make a more precise comparison regarding the wavelength dependence of the fluorescence anisotropy and evaluate the error induced by various experimental factors, we have fitted the anisotropy with mono-exponential functions including a constant C: $r(t) = \beta.\exp(-t/\tau_r) + C$. The fitted parameters β, τ_r and C, depend on the time-window used for the fit, ranging from 3 ps to 7 ps. Despite this variation, the numeric values of the fitted function within the time-window shown in Figure 5, do not change in a significant way and they were found to be reproducible for different experiments. The function r(t) derived from the fluorescence anisotropy of poly(dA).poly(dT) at 330 nm,[11] is shown together with that of $(dA)_{20}.(dT)_{20}$. Over the whole time-scale, the polymer anisotropy is lower than that of the oligomer.

Figure 6

The values of the fitted functions r(t) at 0, 1, 2 and 3 ps, are represented in Figure 6. The size of the circles corresponds to the error bars due to both the experimental reproducibility and the fitting procedure. These plots, although limited to four wavelengths, provide a kind of time-resolved anisotropy spectra. We remark that the highest r(0) value is encountered at the blue part of the spectrum: 0.370 ± 0.020 at 310 nm. At lower energies, the wavelength dependence of r(0) hardly exceeds the error bars. At longer times, a decrease of the anisotropy upon increasing wavelength appears. This trend is quite clear at 3 ps where the anisotropy observed at 420 nm (0.123 ± 0.025) is about half of that determined at 310 nm (0.240 ± 0.025).

Figure 7

The time-resolved fluorescence spectra of $(dA)_{20}.(dT)_{20}$ recorded by the upconversion technique at 0.2 ps (corresponding approximately to the maximum of the fluorescence signal),

1.2 ps and 2.2 ps are presented in Figure 7a with their relative intensities. They are fitted by log-normal curves. The values of ν_{max} and $\Delta\nu$, corresponding to the wavenumber at the maximum and full width at half maximum (fwhm), respectively, are given on Table 3. The maximum of the spectrum shifts slightly towards lower energy as a function of time. The total shift observed within 2 ps (300 cm^{-1}) is somewhat higher than the error (± 100 cm^{-1}). A more important variation is observed in the spectral width, which decreases by 600 cm^{-1} between 0.2 and 1.2 ps and does not exhibit any further change during the next picosecond.

Table 3

In order to depict better the time-evolution of the spectra, we have plotted in Figure 7b the normalized functions $S(\nu)$ together with the steady-state fluorescence spectrum. We observe that the narrowing observed between 0.2 and 1.2 ps, concerns the high energy part of the spectrum. The difference in the spectral width observed between the steady-state spectrum and that recorded at 0.2 ps (600 cm^{-1}) shows that the narrowing takes already place during the rise of the fluorescence signal. This is in line with the observation that the fluorescence decay at 310 nm is more rapid than that at 330 nm (Figure 2, Table 1).

Discussion

A first remark regarding the fluorescence decays of $(dA)_{20}.(dT)_{20}$ is that, they all are slower than those of dAMP (0.13 ps) and TMP (0.64 ps).[10] However, despite their wavelength dependence observed in Figure 2, they all decrease at the same time-scale. This is reflected in the mean values $<\tau_{1\text{-}2}>$ (Table 1), whose variation does not exceed a factor of two. On average, the $<\tau_{1\text{-}2}>$ values are close to the short time-constant determined from the transient absorption signal at 570 nm for $(dA)_{18}.(dT)_{18}$ (1.7 ± 0.3 ps).[15] Although long-lived components have been detected by time-correlated single photon counting in the fluorescence decay of $(dA)_{20}.(dT)_{20}$,[9] their contribution to the amplitude of the signal is extremely weak (<1%). This is also visible in the time-resolved spectra which are quite similar to the steady-state fluorescence spectrum (Figure 7). Considering the significant amplitude of transient absorption signals obtained for the oligomers at times longer than 7 ps,[15,17] it is clear that they correspond to dark states devoid of oscillator strength.

The lengthening of the fluorescence decay determined by upconversion for $(dA)_{20}.(dT)_{20}$ with respect to that of dAMP and TMP, may be due to the fact that the emitting

states are delocalized over two or more bases.[23,24] Exciton states have in general different transition moments and, consequently, different radiative lifetimes than the monomeric chromophores. Nevertheless, judging only from the fluorescence decays, we cannot not preclude that the duplex fluorescence stems from excited states localized on single thymine and/or adenine residues. As a matter of fact, it is possible that steric hindrance within the double helix slows down the non-radiative decay process responsible for the ultrafast internal conversion involving, for example, pyramidalization of the nitrogen atom on position 5 in the case of thymine.[25] Such a modulation is expected to be highly dependent on the local structural parameters, thus giving rise to a large diversity of fluorescence lifetimes.

If we cannot draw a clear conclusion from the fluorescence decays of $(dA)_{20}.(dT)_{20}$ only regarding the localized or delocalized nature of the emitting states, fluorescence anisotropy decays can provide precious information about the excited states involved both in photon absorption and in photon emission. To this end we discuss below the various possible reasons leading to fluorescence depolarization.

Fluorescence anisotropy values lower than 0.4, as those observed in Figure 5, may be simply due to motions of the chromophores. Indeed, very fast motions of the double helix were invoked to explain the low anisotropy values observed by time-correlated single photon counting for $(dA)_{20}.(dT)_{20}$ on the picosecond time-scale.[26] Such an interpretation is in contradiction with more recent studies performed with femtosecond resolution for a DNA double helix containing 2'-aminopurine.[27] This modified base, forming a Watson-Crick pair with thymine, was excited at 330 nm, where the natural bases do not absorb, and, therefore, it is the only emitting chromophore. Under these conditions, it was found that, during a time-scale comparable to that of our own experiments, fluorescence anisotropy remains constant. Consequently, we rule out molecular motions as a possible reason for the decreased anisotropy values determined for $(dA)_{20}.(dT)_{20}$.

At a next step, we examine whether the complex anisotropy patterns shown in Figure 5 can be explained by emission originating from excited states localized on both adenine and thymine residues. Beforehand, we recall that the fluorescence spectrum of dAMP peaks at 306 nm whereas that of TMP at 330 nm. Moreover, the dAMP anisotropy is significantly lower than that of TMP (right panel in Figure 5) because laser excitation at 267 nm populates mainly the S_2 state and emission originates from S_1 state.[4] Thus, if bases absorb and emit photons individually, fluorescence anisotropy should be lower at 310 nm, where the relative contribution of adenine emission is higher compared to the other wavelengths. But just the opposite trend is observed in Figure 5, allowing us to preclude emission from monomeric

adenines. This hypothesis leads to the conclusion that emission stems only from "monomeric" thymines. The same conclusion was reached by Ge and Georgiou from the similarity of the steady-state fluorescence spectra of poly(dA).poly(dT) with that of TMP .[21]

According to the above reasoning, the anisotropy values, noticeably lower than 0.4, observed on Figure 5, constitute the signature of excitation energy transfer occurring within $(dA)_{20}.(dT)_{20}$ already on the sub-picosecond time-scale. Attribution of the fluorescence signals to excited states localized on thymine residues would reveal an unusually efficient Förster transfer. But, as developed in the past by Georgiou et *al.*, Förster transfer among excited states localized on thymines is highly improbable.[26] This is mainly due to the extremely weak overlap between absorption and fluorescence spectra of thymidine chromophores, which is characterized by a Stokes shift as large as 8000 cm^{-1}.

In order to interpret our experimental observations, we propose, as in the case of poly(dA).poly(dT), a model involving Franck-Condon states delocalized over a few bases (excitons). Delocalization is induced by dipolar interactions and/or interactions due to orbital overlap interactions (charge transfer). The fingerprint of those interactions is visible in the steady-state absorption spectrum of $(dA)_{20}.(dT)_{20}$ which is characterized by a weak hypsochromic shift (380 cm^{-1}) of the maximum and an important decrease (*ca.* 30 %) in the maximum molar extinction coefficient (ε_{max}) compared to the sum of the spectra of dAMP and TMP (ε_{max} = 11700 $M^{-1}cm^{-1}$ at 38170 cm^{-1}). Theoretical calculations performed for $(dA)_{10}.(dT)_{10}$, combining the exciton theory with data from quantum chemistry and molecular dynamics simulations, have shown that dipolar coupling induces delocalization of the excited states and causes a weak hypsochromic shift of the spectrum.[24] Moreover, quantum chemical calculations, performed for stacked dimers and pairs of dimers, have explained the hypochromism by the formation of interbase charge transfer states and $\pi\pi^*$ states with partial charge transfer character.[28,29] Although calculations taking into account both types of interactions within extended double helices are not yet available, theoretical studies carried out for other types of systems, have shown that Frenkel excitons and charge transfer excitons may combine.[30]

Given the above picture of the Franck-Condon excited states, the processes underlying our fluorescence upconversion data obtained for $(dA)_{20}.(dT)_{20}$ is described as follows. Laser pulses populate a large number of more or less delocalized excited states. The "large number" is related to both conformation disorder and to homogenous broadening of monomer

electronic transitions.[24] Emission can be viewed as ranging between two limiting cases (Figure 8).

Figure 8

In one case, we have excited states localized on thymines which emit prior to energy transfer. They are characterized by very short lifetimes, high anisotropy values and their relative contribution is more important at shorter wavelengths.

In the other case, we have delocalized excited states forming an exciton band structure. After excitation, the system undergoes very fast intraband scattering and fluorescence arises from excited states located at the lower part of the exciton band which have different polarization from that of the Franck-Condon states. Most of these emitting states are characterized by longer radiative lifetime and are detected at longer wavelengths. When energy transfer involves a large number of transitions orthogonal to an axis, the fluorescence anisotropy is equal to 0.1. Such r(t) values are reported for columnar phases.[31] This is precisely what is observed for the anisotropy determined for $(dA)_{20}.(dT)_{20}$ at 420 nm at 3ps (Figure 6), for which the $\pi\pi^*$ transitions of the bases, and their linear combinations corresponding to excitons, are roughly perpendicular to the helical axis.

From the above discussion it becomes obvious that the time constants resulting from fits of the fluorescence decays with multi-exponential functions (Table 1 and supporting information) have no physical meaning. This is always the case when energy transfer takes place within a low dimensional multichromophoric system.[32]

Size effect: In order to get a clear picture regarding the size effect on the properties of the duplex states, we compare on Table 2 various properties determined for $(dA)_{20}.(dT)_{20}$ and poly(dA).poly(dT) under the same conditions of buffer and ionic strength, and using identical experimental protocols.

We remark that the absorption maximum of the polymer is located at higher energy than that of the oligomer and its molar extinction coefficient is smaller. The relatively stronger hypsochromic shift observed for poly(dA).poly(dT) (470 cm^{-1}) can be explained, in the frame of the exciton theory, by a larger delocalization of the Franck-Condon states. Such an effect may be due to two different factors. One possibility is that a simple increase in the size of duplex allows more chromophores to participate to the exciton states, whose extent in poly(dA).poly(dT) should exceed 20 base-pairs. A numerical study showed that this happens for triphenylene columnar aggregates.[33] However, these columnar aggregates were

characterized by a constant stacking distance and much stronger transition moments than those involved in the examined duplexes. In the duplexes, the average degree of delocalization, calculated taking into account the dipolar coupling alone, ranges between 2 and 6 bases.[23,24] Thus, delocalization beyond 20 base pairs can be achieved only by orbital overlap interactions at least twice as strong compared to dipolar interactions. Another possibility is that an increase in the size of duplex is accompanied by a decrease in the conformational disorder and the stacking distance[18] leading to a stronger electronic coupling (Figure 8). In particular, orbital overlap interactions are very sensitive to small changes in the interchromophore distance and can also modify the degree of hypochromism, which was found to be stronger for the polymer compared to the oligomer (Table 2).

A larger degree of delocalization of the Franck-Condon states is also corroborated by the lower fluorescence anisotropy values observed at 330 nm for the polymer compared with the oligomer. The weaker time-constants $<\tau_{1\text{-}2}>$ found for $(dA)_{20}.(dT)_{20}$ with respect to those of poly(dA).poly(dT), can be explained by a smaller portion of exciton states, with regard to monomer emission, participating to fluorescence of the oligomer.

In conclusion, the excited state behavior of the oligomer resembles, in a qualitative way, to that of the polymer: the experimental observations are interpreted in both cases by Franck-Condon states delocalized over a few bases, ultrafast energy transfer taking place via intraband scattering and fluorescence arising from both localized and delocalized states.[12] However, in a quantitative way, quite noticeable differences are found between the two systems. The spectral and dynamical properties of the excited states, which in principle are determined by the local environment represented by a few bases, are in fact affected significantly by factors extended to much longer distances. It is important to examine whether this size effect, determined for homopolymeric A-T duplexes, is also valid for other base sequences, and evaluate the possible consequence in the formation of UV induced photolesions.

REFERENCES

(1) Pecourt, J.-M. L.; Peon, J.; Kohler, B. *J. Am. Chem. Soc.* **2000**, *122*, 9348.

(2) Gustavsson, T.; Sharonov, A.; Markovitsi, D. *Chem. Phys. Lett.* **2002**, *351*, 195.

(3) Peon, J.; Zewail, A. H. *Chem. Phys. Lett.* **2001**, *348*, 255.

(4) Onidas, D.; Markovitsi, D.; Marguet, S.; Sharonov, A.; Gustavsson, T. *J. Phys. Chem. B* **2002**, *106*, 11367.

(5) Gustavsson, T.; Sarkar, N.; Lazzarotto, E.; Markovitsi, D.; Improta, R. *Chem. Phys. Lett.* **2006**, *429*, 551.

(6) Gustavsson, T.; Sarkar, N.; Lazzarotto, E.; Markovitsi, D.; Barone, V.; Improta, R. *J. Phys. Chem. B* **2006**, *110*, 12843.

(7) Hare, P. M.; Crespo-Hernades, C.; Kohler, B. *Proc. Natl. Acad. Sci.* **2007**, *104*, 435.

(8) Markovitsi, D.; Onidas, D.; Talbot, F.; Marguet, S.; Gustavsson, T.; Lazzarotto, E. *J. Photochem. Photobiol. A: Chem.* **2006**, *183*, 1.

(9) Markovitsi, D.; Talbot, F.; Gustavsson, T.; Onidas, D.; Lazzarotto, E.; Marguet, S. *Nature* **2006**, *441*, E7.

(10) Markovitsi, D.; Sharonov, A.; Onidas, D.; Gustavsson, T. *ChemPhysChem* **2003**, *3*, 303.

(11) Markovitsi, D.; Onidas, D.; Gustavsson, T.; Talbot, F.; Lazzarotto, E. *J. Am. Chem. Soc.* **2005**, *127*, 17130.

(12) Markovitsi, D.; Gustavsson, T.; Talbot, F. *Photochem. & Photobiol. Sci.* **2007**, DOI: 10.1039/b705674e.

(13) Lewis, F. D.; Zhang, L.; Liu, X.; Zuo, X.; Tiede, D. M.; Long, H.; Schatz, G. C. *J. Am. Chem. Soc.* **2005**, 14445.

(14) Lewis, D. F.; Liu, X.; Wu, Y.; Zuo, X. *J. Am. Chem. Soc.* **2003**, *125*, 12729.

(15) Crespo-Hernández, C. E.; Cohen, B.; Kohler, B. *Nature* **2005**, *436*, 1141.

(16) Crespo-Hernández, C. E.; Cohen, B.; Kohler, B. *Nature* **2006**, *441*, E8.

(17) Buchvarov, I.; Wang, Q.; Raytchev, M.; Trifonov, A.; Fiebig, T. *Proc. Natl. Acad. Sci.* **2007**, *104*, 4794.

(18) Zuo, X.; Cui, G.; Merz Jr., K. M.; Zhang, L.; Lewis, F. D.; Tiede, D. M. *Proc. Natl. Acad. Sci.* **2006**, *103*, 3534.

(19) Gustavsson, T.; Sharonov, A.; Onidas, D.; Markovitsi, D. *Chem. Phys. Lett.* **2002**, *356*, 49.

(20) Gustavsson, T.; Cassara, L.; Gulbinas, V.; Gurzadyan, G.; Mialocq, J.-C.; Pommeret, S.; Sorgius, M.; van der Meulen, P. *J. Phys. Chem. A* **1998**, *102*, 4229.

(21) Ge, G.; Georghiou, S. *Photochem. Photobiol.* **1991**, *54*, 477.

(22) Ge, G.; Georghiou, S. *Photochem. Photobiol.* **1991**, *54*, 301.

(23) Bouvier, B.; Dognon, J. P.; Lavery, R.; Markovitsi, D.; Millié, P.; Onidas, D.; Zakrzewska, K. *J. Phys. Chem. B* **2003**, *107*, 13512.

(24) Emanuele, E.; Markovitsi, D.; Millié, P.; Zakrzewska, K. *ChemPhysChem* **2005**, *6*, 1387.

(25) Gustavsson, T.; Banyasz, A.; Lazzarotto, E.; Markovitsi, D.; Scalmani, G.; Frisch, M. J.; Barone, V.; Improta, R. *J. Am. Chem. Soc.* **2006**, *128*, 607.

(26) Georghiou, S.; Bradrick, T. D.; Philippetis, A.; Beechem, J. *Biophys. J.* **1996**, *70*, 1909.

(27) Pal, S. K.; Zhao, L.; Xia, T.; Zewail, A. H. *Proc. Natl. Acad. Sci. USA* **2003**, *100*, 13746.

(28) Starikov, E. B. *Modern Phys. Lett. B* **2004**, *18*, 825.

(29) Varsano, D.; Di Felice, R.; Marques, M. A. L.; Rubio, A. *J. Phys. Chem. B* **2006**, *110*, 7129.

(30) Mančal, T.; Valkunas, L.; Fleming, G. R. *Chem. Phys. Lett.* **2006**, *432*, 301.

(31) Markovitsi, D.; Germain, A.; Millie, P.; Lécuyer, I.; Gallos, L.; Argyrakis, P.; Bengs, H.; Ringsdorf, H. *J. Phys. Chem.* **1995**, *99*, 1005.

(32) Blumen, A.; Klafter, J.; Zumofen, G. Models for reaction dynamics in glasses. In *Optical spectroscopy of glasses*; Zschokke, I., Ed.; Reidel Publishing Co., 1986; pp 199.

(33) Marguet, S.; Markovitsi, D.; Millié, P.; Sigal, H.; Kumar, S. *Journal of Physical Chemistry B* **1998**, *102*, 4697.

(34) Riley, M.; Maling, B.; Chamberling, M. J. *J. Mol. Biol.* **1966**, *20*, 359.

Table 1: Parameters derived from the fit of the fluorescence decays of $(dA)_{20}.(dT)_{20}$ using bi-exponential functions $F(t) = \alpha.\exp(-t/\tau_1) + (1-\alpha).\exp(-t/\tau_2)$. The average lifetime is defined as $\langle\tau_{1\text{-}2}\rangle = \alpha\cdot\tau_1 + (1-\alpha)\cdot\tau_2$. The error bars result from the fits.

λ (nm)	**α**	**τ_1 (ps)**	**τ_2 (ps)**	**$\langle\tau_{1\text{-}2}\rangle$ (ps)**
310	0.78 ± 0.01	0.34 ± 0.02	2.24 ± 0.10	0.75 ± 0.03
330	0.66 ± 0.01	0.46 ± 0.01	2.80 ± 0.05	1.26 ± 0.02
380	0.76 ± 0.01	0.48 ± 0.02	3.83 ± 0.12	1.27 ± 0.03
420	0.81 ± 0.01	0.52 ± 0.03	6.08 ± 0.63	1.57 ± 0.12

Table 2

Comparison of the optical properties of $(dA)_{20}.(dT)_{20}$ and poly(dA).poly(dT) determined in phosphate buffer (pH=6.8; 0.1 M NaH_2PO_4, 0.1 M Na_2HPO_4, 0.25 M NaCl) following the same experimental protocols; $\nu_{max,abs}$ and $\nu_{max,fl}$: wavenumbers corresponding to the maxima of the steady-state absorption and fluorescence spectra, respectively; ε_{max}: maximum molar extinction coefficient; $<\tau_{1-2}>_{\lambda}$: average lifetime determined by fluorescence upconversion at wavelength λ; $r(t)_{330nm}$ fluorescence anisotropy at time t (ps) and 330 nm.

property	**$(dA)_{20}.(dT)_{20}$**	**poly(dA).poly(dT)**
$\nu_{max,\ abs}$ (cm^{-1})	38550 ± 30	38640 ± 30
ε_{max} ($M^{-1}cm^{-1}$)[a]	7900[b]	6000 [c]
$\nu_{max,\ fl}$ (cm^{-1})	30600 ± 100	30900 ± 100
$<\tau_{1-2}>_{330nm}$ (ps)	1.3	2.1
$<\tau_{1-2}>_{380nm}$ (ps)	1.3	2.5
$<\tau_{1-2}>_{420nm}$ (ps)	1.6	3.0
$r(0)_{330nm}$	0.31	0.28
$r(3)_{330nm}$	0.23	0.18

a) per base b) see supporting information c) from reference [34].

Table 3: Parameters derived from the fit of the fluorescence time-resolved spectra of $(dA)_{20}.(dT)_{20}$, recorded by fluorescence upconversion, using log-normal functions. Error: ± 100 cm^{-1}; ν_{max} and $\Delta\nu$, correspond to the wavenumber at the maximum and full width at half maximum (fwhm),

t (ps)	ν_{max} (cm^{-1})	$\Delta\nu$ (cm^{-1})
Steady-state	30600	6900
0.2	30800	5700
1.2	30700	5100
2.2	30500	5200

Figure 1

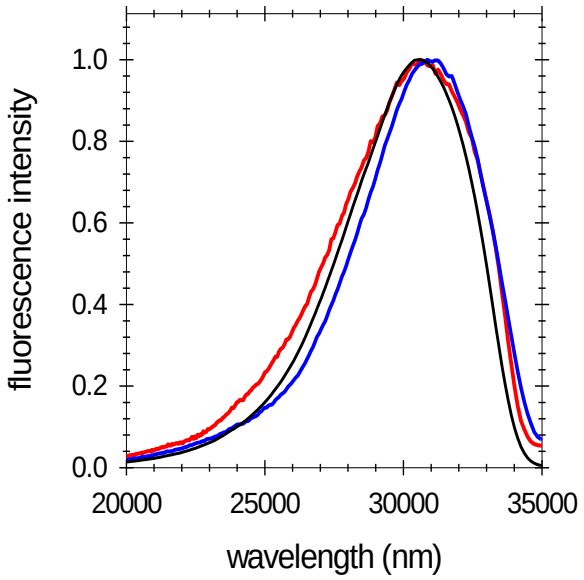

Steady-state fluorescence spectra of $(dA)_{20}.(dT)_{20}$ (red), poly(dA).poly(dT) (blue) and TMP (black) recorded following excitation at 267 nm.

Figure 2

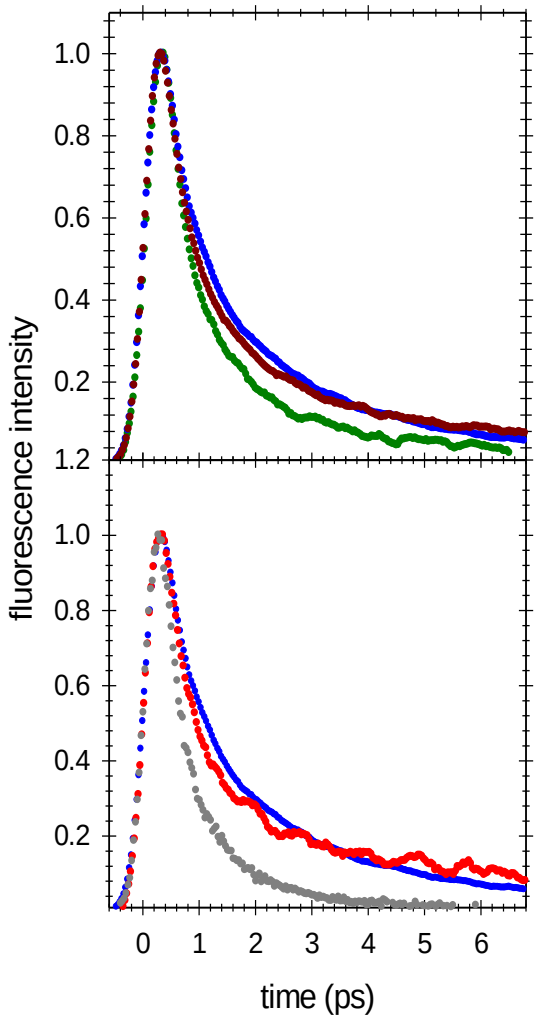

Normalized fluorescence decays of $(dA)_{20}.(dT)_{20}$ at 310 nm (green), 330 nm (blue), 380 nm (claret) and 420 nm (red). The decay of an equimolar mixture of dAMP and TMP (grey) at 330 nm is also shown for comparison. Excitation wavelength: 267 nm. In order to make the comparison easier, signals were smoothed by averaging arithmetically five consecutive data points.

Figure 3

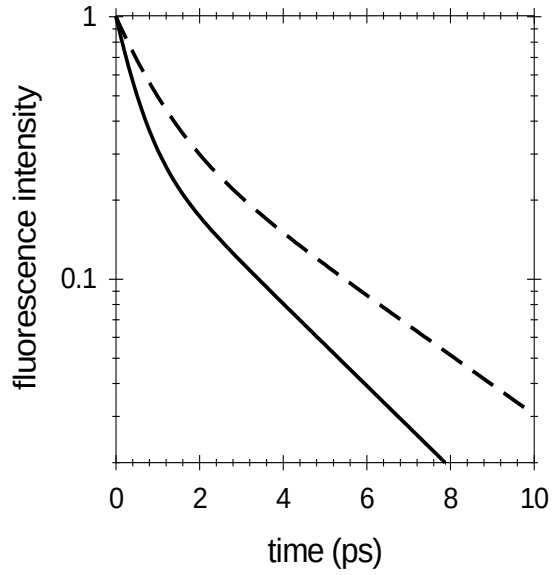

Bi-exponential model functions resulting from a fitting/deconvolution procedure of the fluorescence decays recorded for $(dA)_{20}.(dT)_{20}$ (solid line) and poly(dA).poly(dT) (dashed line) at 330 nm following excitation at 267 nm.

Figure 4

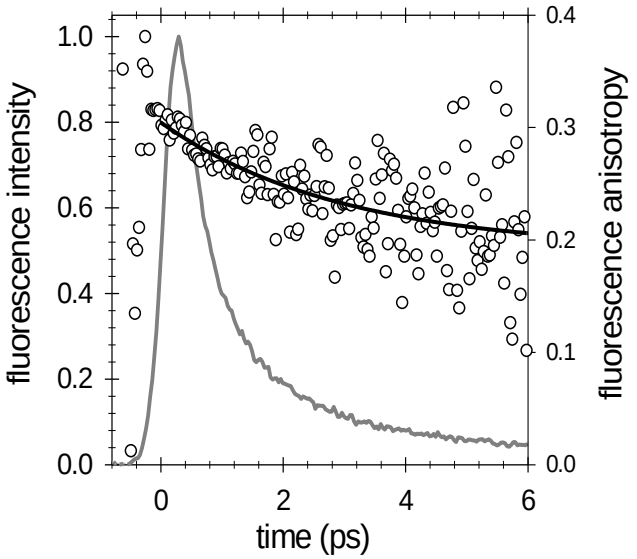

Fluorescence decay (grey) and fluorescence anisotropy decay (circles) of $(dA)_{20}.(dT)_{20}$ at 330 nm. Excitation wavelength: 267 nm. The black line corresponds to the fit of the fluorescence anisotropy decay with a mono-exponential function: $r(t) = \beta.\exp(-t/\tau_r) + C$.

Figure 5

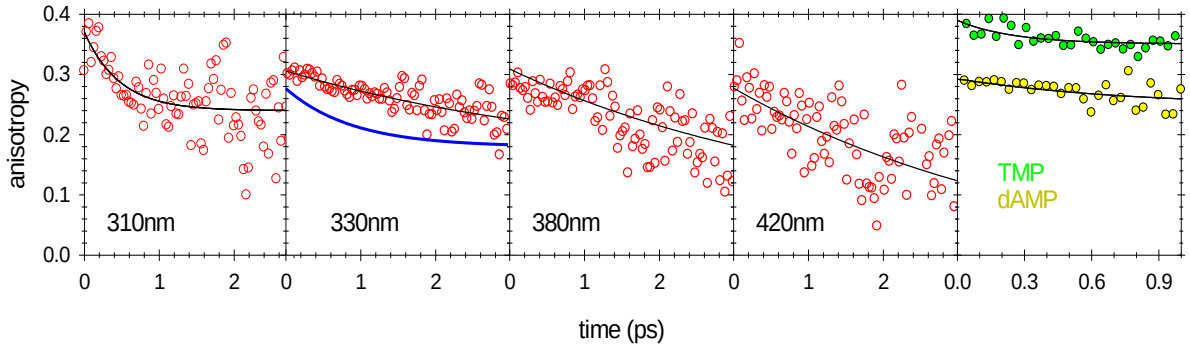

Fluorescence anisotropy decays determined for $(dA)_{20}.(dT)_{20}$ at 310, 330, 380 and 420 nm (red). Right panel: fluorescence anisotropy decays of dAMP (yellow) and TMP (green), which do not vary at the probed wavelengths. Excitation wavelength: 267 nm. The black lines correspond to the fit with mono-exponential functions $r(t) = \beta.\exp(-t/\tau_r) + C$. The blue line at 330 nm corresponds to the fit of the fluorescence anisotropy decay determined for poly(dA).poly(dT).[11]

Figure 6

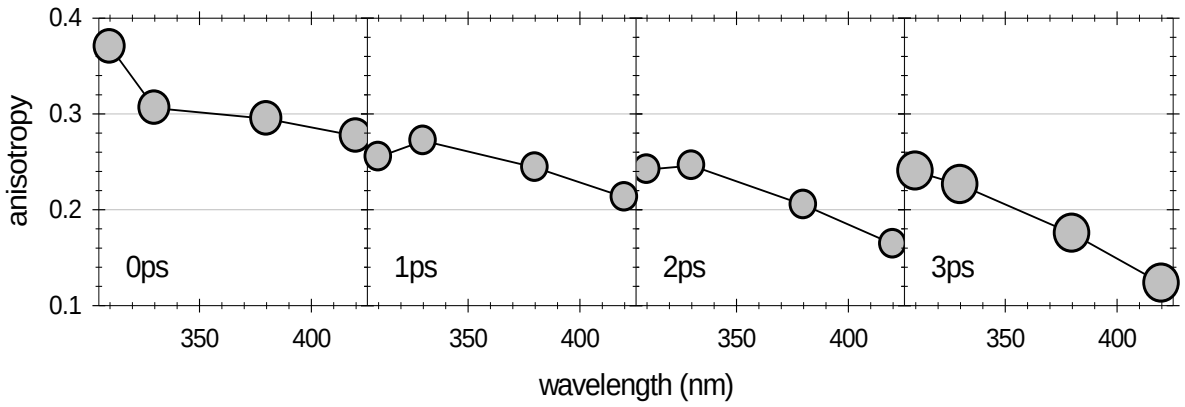

Time-resolved "fluorescence anisotropy spectra" determined for $(dA)_{20}.(dT)_{20}$ following excitation at 267 nm. They are constructed using the r(t) functions fitting the fluorescence anisotropies. The diameter of the circles corresponds to the error bars resulting from both the reproducibility of the experiments and the fitting procedure.

Figure 7

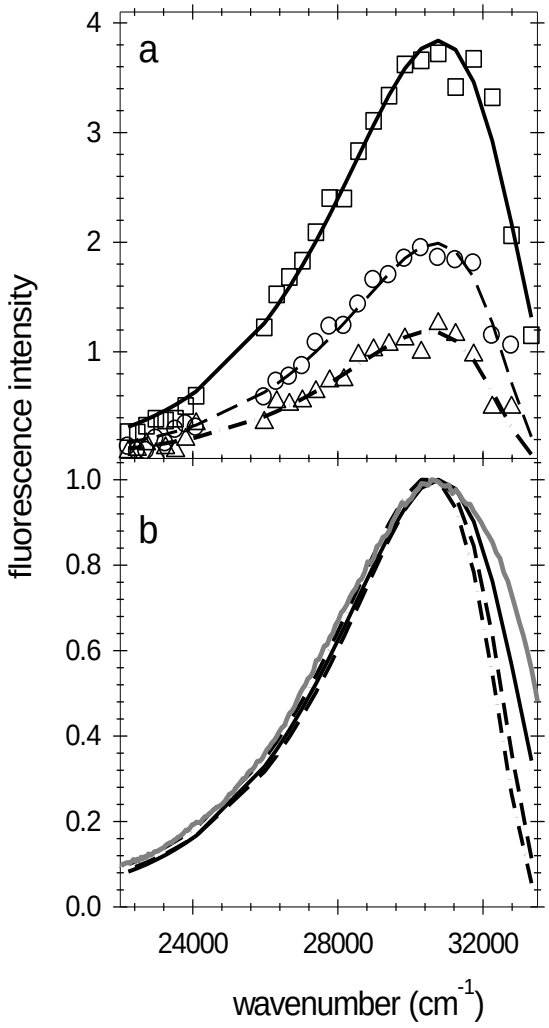

Time-resolved fluorescence spectra recorded for $(dA)_{20}.(dT)_{20}$ at 0.2 ps (squares), 1.2 ps (circles) and 2.2 ps (triangles). The experimental spectra are fitted with log-normal curves S(ν) (solid, dashed and dashed-dotted lines, respectively). In (a), the spectra are represented with their relative intensities. In (b), the fitted functions S(ν) are normalized and compared to the steady-state fluorescence spectrum (grey). Excitation wavelength: 267 nm.

Figure 8

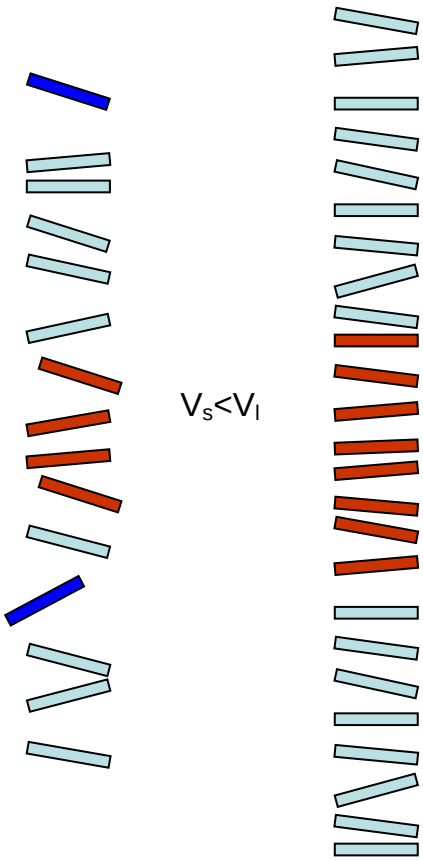

Schematic representation of the size effect on the extent of exciton states (in red). For simplicity, only two stacks of chromophores with different aggregation numbers are represented. The small aggregate (left) is characterized by more important disorder compared to the larger aggregate (right). Consequently, the average coupling strength corresponding to the small aggregate (V_s) is weaker than that corresponding to the large one (V_l), and gives rise to less delocalized excited states. In blue are shown chromophores which may behave a "monomers".